

# 1 PyDamage: automated ancient damage 2 identification and estimation for contigs in 3 ancient DNA *de novo* assembly

4 Maxime Borry<sup>1</sup>, Alexander Hübner<sup>1,2</sup>, A.B. Rohrlach<sup>3,4</sup>, and Christina  
5 Warinner<sup>1,2,5</sup>

6 <sup>1</sup>Microbiome Sciences Group, Department of Archaeogenetics, Max Planck Institute for  
7 the Science of Human History, Jena, Germany, Kahlaische Straße 10, 07445 Jena

8 <sup>2</sup>Faculty of Biological Sciences, Friedrich-Schiller University, Jena, Germany, 07743

9 <sup>3</sup>Population Genetics Group, Department of Archaeogenetics, Max Planck Institute for  
10 the Science of Human History, Jena, Germany, Kahlaische Straße 10, 07445 Jena

11 <sup>4</sup>ARC Centre of Excellence for Mathematical and Statistical Frontiers, The University of  
12 Adelaide, Adelaide SA 5005, Australia

13 <sup>5</sup>Department of Anthropology, Harvard University, Cambridge, MA, USA 02138

14 Corresponding author:

15 Maxime Borry, Christina Warinner

16 Email address: borry@shh.mpg.de, warinner@fas.harvard.edu

## 17 ABSTRACT

18 DNA *de novo* assembly can be used to reconstruct longer stretches of DNA (contigs), including genes  
19 and even genomes, from short DNA sequencing reads. Applying this technique to metagenomic data  
20 derived from archaeological remains, such as paleofeces and dental calculus, we can investigate past  
21 microbiome functional diversity that may be absent or underrepresented in the modern microbiome  
22 gene catalogue. However, compared to modern samples, ancient samples are often burdened with  
23 environmental contamination, resulting in metagenomic datasets that represent mixtures of ancient and  
24 modern DNA. The ability to rapidly and reliably establish the authenticity and integrity of ancient samples  
25 is essential for ancient DNA studies, and the ability to distinguish between ancient and modern sequences  
26 is particularly important for ancient microbiome studies. Characteristic patterns of ancient DNA damage,  
27 namely DNA fragmentation and cytosine deamination (observed as C-to-T transitions) are typically used  
28 to authenticate ancient samples and sequences. However, existing tools for inspecting and filtering aDNA  
29 damage either compute it at the read level, which leads to high data loss and lower quality when used  
30 in combination with *de novo* assembly, or require manual inspection, which is impractical for ancient  
31 assemblies that typically contain tens to hundreds of thousands of contigs. To address these challenges,  
32 we designed PyDamage, a robust, automated approach for aDNA damage estimation and authentication  
33 of *de novo* assembled aDNA. PyDamage uses a likelihood ratio based approach to discriminate between  
34 truly ancient contigs and contigs originating from modern contamination. We test PyDamage on both  
35 simulated, and empirical aDNA data from archaeological paleofeces, and we demonstrate its ability  
36 to reliably and automatically identify contigs bearing DNA damage characteristic of aDNA. Coupled  
37 with aDNA *de novo* assembly, PyDamage opens up new doors to explore functional diversity in ancient  
38 metagenomic datasets.

## 39 INTRODUCTION

40 Ancient DNA (aDNA) is highly fragmented (Orlando et al., 2021; Warinner et al., 2017). Although  
41 genomic DNA molecules within a living organism can be millions to hundreds of millions of base pairs  
42 (bp) long, postmortem enzymatic and chemical degradation after death quickly reduces DNA to fragment  
43 lengths of less than 150 bp, typically with medians less than 75 bp and modes less than 50 bp (Mann et al.,  
44 2018; Hansen et al., 2017). Within the field of metagenomics, many approaches require longer stretches  
45 of DNA for adequate analysis, a requirement that particularly applies to functional profiling, which often

46 involves *in silico* translation steps (Seemann, 2014). For example, FragGeneScan (Rho et al., 2010), a tool  
47 designed for gene prediction from short read data, fails to predict open-reading frames in DNA sequences  
48 shorter than 60 bp. If applied directly to highly fragmented ancient metagenomic datasets, such data  
49 filtering can introduce biases that interfere with functional analyses when preservation is variable across  
50 samples or when comparing ancient samples to modern ones.

51 Because very short (<100 bp) and ultrashort (<50 bp) DNA molecules pose many downstream  
52 analytical challenges, there is a long-standing interest in leveraging the approach of *de novo* assembly  
53 to computationally reconstruct longer stretches of DNA for analysis. With *de novo* assembly, longer  
54 contiguous DNA sequences (contigs), and sometimes entire genes or gene clusters, can be reconstructed  
55 from individual sequencing reads (Compeau et al., 2011), which can then be optionally binned into  
56 metagenome-assembled genomes (MAGs) (Kang et al., 2015). Such contigs are more amenable to  
57 functional profiling, and applying this technique to microbial metagenomics datasets derived from  
58 archaeological remains, such as paleofeces and dental calculus, has the potential to reveal ancient genes  
59 and functional diversity that may be absent or underrepresented in modern microbiomes (Tett et al., 2019;  
60 Wibowo et al., 2021; Brealey et al., 2020). However, because ancient samples generally contain a mixture  
61 of ancient bacterial DNA and modern bacterial contaminants, it is essential to distinguish, among the  
62 thousands of contigs generated by assembly, truly ancient contigs from contigs that may originate from  
63 the modern environment, such as the excavation site, storage facility, or other exogenous sources.

64 In addition to being highly fragmented, aDNA also contains other forms of characteristic molecular  
65 decay, namely cytosine deamination (observed as C-to-T transitions in aDNA datasets) (Dabney et al.,  
66 2013), which can be measured and quantified to indicate the authenticity of an ancient sample, or even  
67 an individual sequence (Hofreiter et al., 2001; Briggs et al., 2007b). However, tools for inspecting and  
68 filtering aDNA damage were primarily designed for genomic and not metagenomic applications, and  
69 they are largely unsuited or impractical for use in combination with *de novo* assembly. For example,  
70 PMDTools (Skoglund et al., 2014) operates at the read level, and when subsequently combined with *de*  
71 *novo* assembly leads to higher data loss and lower overall assembly quality. MapDamage (Ginolhac et al.,  
72 2011) and DamageProfiler (Neukamm et al., 2020) are tools that can be applied to assembled contigs, but  
73 require manual contig inspection by the user, which is infeasible for *de novo* assemblies yielding tens to  
74 hundreds of thousands of contigs. Other tools, such as mapDamage2 (Jónsson et al., 2013), do provide an  
75 estimation of damage, but use slower algorithms that do not scale well to the analysis of many thousands  
76 of contigs. A faster, automated approach with a better sensitivity for distinguishing truly ancient contigs  
77 from modern environmental contigs is needed.

78 Here, we present PyDamage, a software tool to automate the process of contig damage identification  
79 and estimation. PyDamage models aDNA damage from deamination data (C-to-T transitions), and tests  
80 for damage significance using a likelihood ratio test to discriminate between truly ancient contigs and  
81 contigs originating from modern contaminants. Testing PyDamage on *in silico* simulated data, we show  
82 that it is able to accurately distinguish ancient and modern contigs. We then apply PyDamage to *de novo*  
83 assembled DNA from ancient paleofeces from the site of Cueva de los Muertos Chiquitos, Mexico (ca.  
84 1300 BP) and find that the contigs PyDamage identifies as ancient are consistent with taxa known to be  
85 members of the human gut microbiome. Among the ancient contigs, PyDamage authenticated multiple  
86 functional genes of interest, including a multidrug and bile salt resistance gene cluster from the gut  
87 microbe *Treponema succinifaciens*, a species that is today only found in societies practicing traditional  
88 forms of subsistence. Using PyDamage, *de novo* assembled contigs from aDNA datasets can be rapidly  
89 and robustly authenticated for a variety of downstream metagenomics applications.

## 90 MATERIAL AND METHODS

### 91 Simulated sequencing data

92 In order to evaluate the performance of PyDamage with respect to the GC content of the assembled  
93 genome, the sequencing depth along the genome, the amount of observed aDNA damage on the DNA  
94 fragments, and the mean length of these DNA fragments, we simulated short-read sequencing data  
95 using gargamel (Renaud et al., 2017) varying these four parameters. We chose three microbiome-  
96 associated microbial taxa with low (*Methanobrevibacter smithii*, 31%), medium (*Tannerella forsythia*,  
97 47%), and high (*Actinomyces dentalis*, 72%) GC content, following Mann et al. (2018) (Figure 1a). Using  
98 three different read length distributions (Figure 1b), we generated short-read sequencing data from each  
99 reference genome using gargamel's *fragSim*. To the resulting short-read sequences we added different

100 amounts of aDNA damage using gargammel's *deamSim* so that ten levels of damage ranging from 0% to  
101 20% were observed, which were measured as the amount of observed C-to-T substitutions on the terminal  
102 base at the 5' end of the DNA fragments (Figure 1c). Finally, each of these 90 simulated datasets was  
103 subsampled to generate nine coverage bins ranging from 1-fold to 500-fold genome coverage by randomly  
104 drawing a coverage value from the uniform distribution defining each bin (Figure 1d) and these were  
105 aligned to their respective reference genome using BWA *aln* (Li and Durbin, 2009) with the non-default  
106 parameters optimized for aDNA *-n 0.01 -o 2 -l 16500* (Meyer et al., 2012).

107 Test contigs of different length were simulated by defining nine contig length bins ranging from 0.5  
108 kb to 500 kb length (Figure 1e) and randomly drawing 100 contig lengths from the respective uniform  
109 distribution defining each bin. Next, we chose the location of these test contigs by randomly selecting a  
110 contig from all contigs of sufficient length. We determined the exact location on the selected test contig  
111 from the reference genome by randomly drawing the start position from the uniform distribution defined  
112 by the length of the selected reference contig. This resulted in 900 test contigs per reference genome.  
113 Using these test contigs, we selected the aligned DNA fragments of the simulated sequencing data that  
114 overlapped the region defined by the contig and evaluated them using PyDamage. In total, we evaluated  
115 702,900 test contigs (243,000 contigs for both *M. smithii* and *T. forsythia*, and 216,000 contigs for *A.  
116 dentalis*, for which no reference contig longer than 200 kb was available).

## 117 **Archaeological sample**

### 118 **Preparation and sequencing**

119 We re-analyzed ancient metagenomic data from the archaeological paleofeces sample ZSM028 (Zape 28)  
120 dating to ca. 1300 BP from the site of Cueva de los Muertos Chiquitos, in Mexico, previously published in  
121 Borry et al. (2020) (ENA run accession codes ERR3678595, ERR3678598, ERR3678602, ERR3678603,  
122 and ERR3678613).

### 123 **Bioinformatic processing**

124 The ZSM028 sample was first trimmed to remove adapters, low quality sequences with Q-scores below  
125 20, and short sequences below 30 bp using AdapterRemoval (Schubert et al., 2016) v2.3.1. The reads  
126 were *de novo* assembled into contigs using MetaSPAdes Nurk et al. (2017) v3.13.1 using the non-default  
127 k-mer lengths 21, 33, and 45. Reads were then mapped back to the contigs with length > 1,000 bp  
128 using Bowtie2 (Langmead and Salzberg, 2012), in the very-sensitive mode, while allowing up to 1  
129 mismatch in the seeding process. The alignment files were then given as an input to PyDamage v0.50.  
130 Contigs passing filtering thresholds were functionally annotated with Prokka v1.14.6 (Seemann, 2014),  
131 using the --metagenome flag.

### 132 **Contig Taxonomic Profiling**

133 To investigate the taxonomic profile of the contigs that passed the PyDamage filtering, we ran Kraken2  
134 v2.1.1 (Wood et al., 2019) using the PlusPFP database ([https://benlangmead.github.io/  
135 aws-indexes/k2](https://benlangmead.github.io/aws-indexes/k2)) from 27/1/2021. We then generated the Sankey plot using Pavian (Breitwieser and  
136 Salzberg, 2016).

### 137 **PyDamage implementation**

PyDamage takes alignment files of reads (in SAM, BAM, or CRAM format) mapped against reference  
sequences (*i.e.*, contigs, a MAG, a genome, or any other reference sequences of DNA). For each read  
mapping to each reference sequence  $j$ , using pysam (pysam developers, 2018), we count the number of  
apparent C-to-T transitions at each position which is  $i$  bases from the 5' terminal end,  $i \in \{0, 1, \dots, k\}$ ,  
denoted  $N_i^j$  (by default, we set  $k=35$ ). Similarly we denote the number of observed conserved 'C-to-C'  
sites  $M_i^j$ , thus

$$M^j = (M_0^j, \dots, M_k^j) \quad \text{and} \quad N^j = (N_0^j, \dots, N_k^j).$$

138 Finally, we calculate the proportion of C-to-T transitions occurring at each position, denoted  $p_i^j$ , in the  
139 following way:

$$\hat{p}_i^j = \frac{N_i^j}{M_i^j + N_i^j}.$$

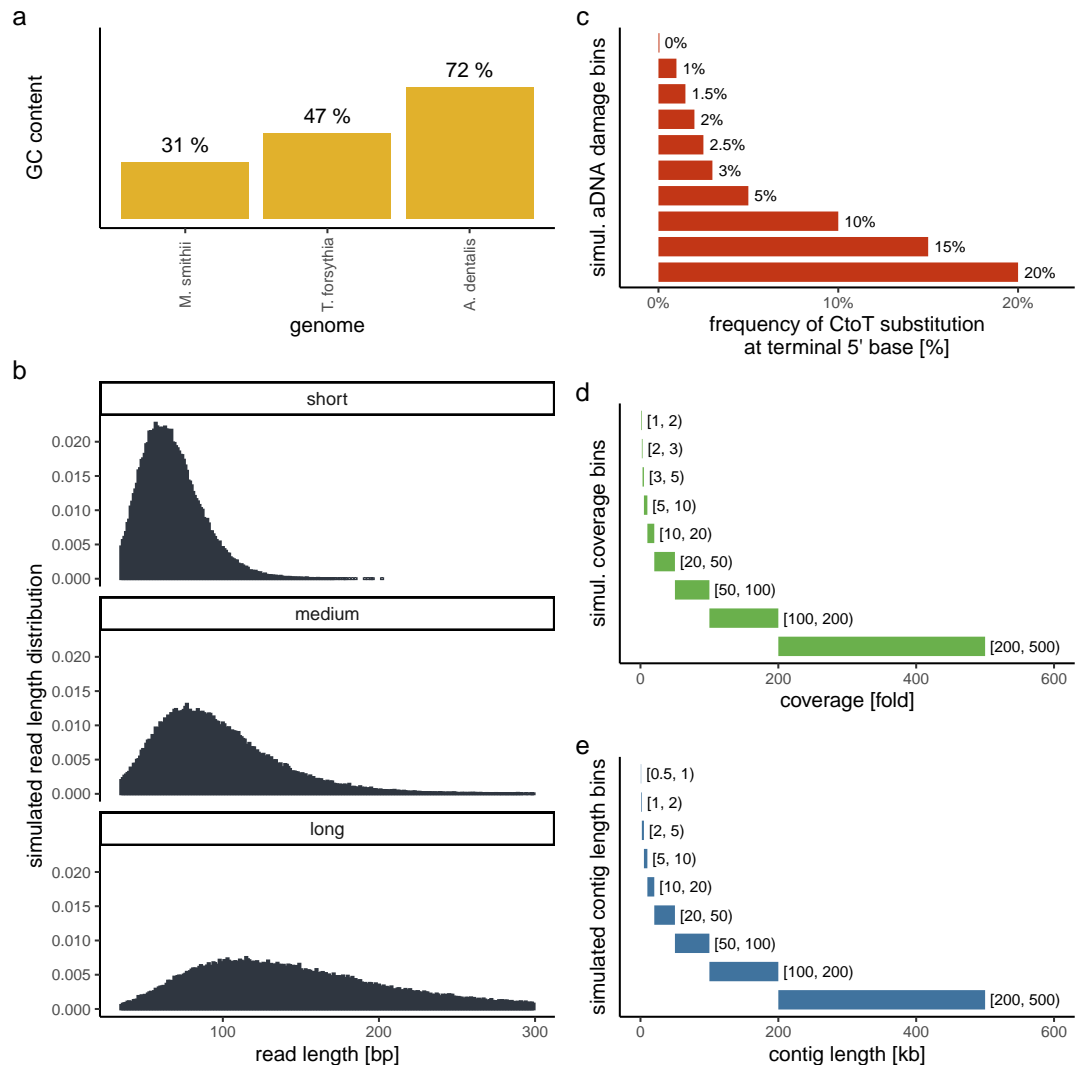


**Figure 1. Simulation scheme for evaluating the performance of PyDamage.** **a** The GC content of the three microbial reference genomes. **b** The read length distributions used as input into *gargammel fragSim*. **c** The amount of aDNA damage as observed as the frequency of C-to-T substitutions on the terminal 5' end of the DNA fragments that was added using *gargammel deamSim*. **d** Nine coverage bins from which the exact coverage was sampled by randomly drawing a number from the uniform distribution defining the bin. **e** Nine contig length bins from which the exact contig length was sampled by randomly drawing a number from the uniform distribution defining the bin.

140 For  $D_i$ , the event that we observe a C-to-T transition  $i$  bases from the terminal end, we define two  
 141 models: a null model  $\mathcal{M}_0$ (equation 1) which assumes that damage is independent of the position from the  
 142 5' terminal end, and a damage model  $\mathcal{M}_1$  (equation 2) which assumes a decreasing probability of damage  
 143 the further a the position from the 5' terminal end. For the damage model, we re-scale the curve to the  
 144 interval defined by parameters  $[d_{pmin}^j, d_{pmax}^j]$ .

$$P_0(D_i | p_0, j) = p_0 = \mathcal{M}_0 \pi^j, \quad (1)$$

$$\begin{aligned} P_1(D_i | p_d^j, d_{pmin}^j, d_{pmax}^j, j) &= \frac{\left( [(1-p_d^j)^i \times p_d^j] - \hat{p}_{min}^j \right)}{\hat{p}_{max}^j - \hat{p}_{min}^j} \times (d_{pmax}^j - d_{pmin}^j) + d_{pmin}^j \\ &= \mathcal{M}_1 \pi_i^j, \end{aligned} \quad (2)$$

where

$$\hat{p}_{min}^j(p_d^j) = (1-p_d^j)^k \times p_d^j \quad \text{and} \quad \hat{p}_{max}^j(p_d^j) = (1-p_d^j)^0 \times p_d^j.$$

Using the curve fitting function of Scipy (Virtanen et al., 2020), with a `trf` (Branch et al., 1999) optimization and a Huber loss (Huber, 1992), we optimize the parameters of both models using  $p_i^j$ , by minimising the sum of squares, giving us the optimized set of parameters

$$\hat{\theta}_0 = \{\hat{p}_0\} \quad \text{and} \quad \hat{\theta}_1 = \{\hat{p}_d^j, \hat{d}_{pmin}^j, \hat{d}_{pmax}^j\}$$

for  $\mathcal{M}_0$  and  $\mathcal{M}_1$  respectively. Under  $\mathcal{M}_0$  and  $\mathcal{M}_1$  we have the following likelihood functions

$$\begin{aligned} \mathcal{L}_0(\hat{\theta}_0 | M^j, N^j) &= \prod_{i=0}^k \binom{M_i^j + N_i^j}{N_i^j} \left( \mathcal{M}_0 \hat{\pi}^j \right)^{N_i^j} \left( 1 - \mathcal{M}_0 \hat{\pi}^j \right)^{M_i^j}, \\ \mathcal{L}_1(\hat{\theta}_1 | M^j, N^j) &= \prod_{i=0}^k \binom{M_i^j + N_i^j}{N_i^j} \left( \mathcal{M}_1 \hat{\pi}_i^j \right)^{N_i^j} \left( 1 - \mathcal{M}_1 \hat{\pi}_i^j \right)^{M_i^j}, \end{aligned}$$

where  $\mathcal{M}_0 \hat{\pi}^j$  and  $\mathcal{M}_1 \hat{\pi}_i^j$  are calculated using equations 1 and 2. Note that if  $d_{pmax}^j = d_{pmin}^j = p_0$ , then  $\mathcal{M}_0 \pi^j = \mathcal{M}_1 \pi_i^j$  for  $i = 0, \dots, k$ . Hence to compare the goodness-of-fit for models  $\mathcal{M}_0$  and  $\mathcal{M}_1$  for each reference, we calculate a likelihood-ratio test-statistic of the form

$$\lambda_j = -2 \ln \left[ \frac{\mathcal{L}_0(\hat{\theta}_0 | M^j, N^j)}{\mathcal{L}_1(\hat{\theta}_1 | M^j, N^j)} \right],$$

from which we compute a *p*-value using the fact that  $\lambda_j \sim \chi_2^2$ , asymptotically. Finally, we adjust the *p*-values for multiple testing of all references, using the StatsModels (Seabold and Perktold, 2010) implementation of the Benjamini-Hochberg procedure (Benjamini and Hochberg, 1995).

## RESULTS

### Statistical Analysis and Model Selection

To test the performance of PyDamage in recognizing metagenome-assembled contigs with ancient DNA damage, we used the simulated short-read sequencing data aligned against simulated contigs of different lengths. Our method correctly identified contigs as not significantly damaged for simulations with no damage in 100% of cases. However, our model only correctly identified contigs as significantly damaged in 87.71% of cases where the contigs were simulated to have damage. To assess the performance of our method, and to determine the simulation parameters that most affected model accuracy, we analysed the simulated data using logistic regression via the `glm` function as implemented in the stats package using R (R Core Team, 2018). We included as potential explanatory variables the median read length, the simulated coverage, the simulated contig length, the simulated level of damage, and the GC content of each of the reference contigs, yielding 32 candidate logistic regression models.

We separated the data into two data sets: half of our data was used as ‘fit data’, data for performing model fit and parameter estimation, and the remaining half was reserved as ‘test data’, data that is used to assess model accuracy on data not used in fitting the model ( $n = 206,831$  in both cases). Unfortunately, with so many observations in our model, classical model selection methods such as AIC and ANOVA tend to overfit (Babyak, 2004). Instead, for each of the fitted 32 logistic regression models (with  $\varepsilon = 1 \times 10^{-14}$  and maximum iterations  $10^3$ ) we calculated the ‘balanced accuracy’ (the average of the sensitivity and the

167 specificity) and Nagelkerke's  $R^2$ . We chose the balanced accuracy to equally weight the importance of  
168 detecting true damage when it is present, and to also reject a false identification of damage when it is not  
169 present.

170 Of the 32 candidate models, four models had the highest  $R^2$  between 0.556 and 0.568 (compared to  
171 the next greatest of 0.429, see Table 1). Of these four models, the maximum balanced accuracy belonged  
172 to the model which had the following predictor variables: contig length, mean coverage, GC content  
173 and the simulated level of damage, although these values were extremely close for all four models (see  
174 Figure 2). Because it is possible that there is correlation between some of our predictor variables (*i.e.*  
175 increased levels of simulated damage could lead to a reduced median read length), we then performed a  
176 Relative Weights Analysis (RWA) to further estimate predictor variable importance in an uncorrelated  
177 setting (Chan, 2020). In essence, RWA calculates the proportion of the overall  $R^2$  for the model that  
178 can be attributed to each variable. We performed RWA on both the full model and our best performing  
179 model. We found that the median read length and GC content accounted for only 0.31% and 2.75%  
180 of the  $R^2$  value in the full model respectively. However, we found that contig length, mean coverage  
181 and the simulated level of damage all accounted for approximately one third of the  $R^2$  value in our best  
182 performing model, indicating that these are the predictor variables of importance.

Variables	Balanced Accuracy	$R^2$
damage/contiglength/GCcontent/readlength/coverage	0.495	0.568
damage/contiglength/GCcontent/coverage	0.496	0.566
damage/contiglength/readlength/coverage	0.492	0.557
<b>damage/contiglength/coverage</b>	<b>0.493</b>	<b>0.556</b>
contiglength/GCcontent/readlength/coverage	0.429	0.429
contiglength/GCcontent/coverage	0.430	0.428
contiglength/readlength/coverage	0.421	0.420
contiglength/coverage	0.422	0.419
damage/contiglength/GCcontent/readlength	0.574	0.378
damage/contiglength/GCcontent	0.581	0.377

**Table 1.** Balanced accuracy and Nagelkerke's  $R^2$  values for the top ten models (as measured by  $R^2$ ). The model we retained is highlighted in bold.

183 Our final logistic regression model identified mean coverage, the level of damage, and the contig length  
184 as significant predictor variables for model accuracy. Each of these variables had positive coefficients,  
185 meaning that an increase in damage, genome coverage, or contig length all lead to improved model  
186 accuracy. Each variable contributed about one third weight to the  $R^2$  value in the model, indicating  
187 roughly equal importance in the accuracy of PyDamage. We integrated the best logistic regression model  
188 in PyDamage, with the StatsModels (Seabold and Perktold, 2010) implementation of GLM to provide an  
189 estimation of PyDamage ancient contig prediction accuracy given the amount of damage, coverage, and  
190 length for each reference (Figure 3), and found these predictions to adequately match the observed model  
191 accuracy for our simulated data set (Figure 4).

## 192 Application of PyDamage to Archeological samples

193 To test PyDamage on empirical data, we assembled metagenomic data from the paleofeces sample  
194 ZSM028 with the metaSPAdes *de novo* assembler. We obtained a total of 359,807 contigs, with an  
195 N50 of 429 bp. Such assemblies, consisting of a large number of relatively short contigs, are typical  
196 for *de novo* assembled aDNA datasets (Wibowo et al., 2021). After filtering for sequences longer than  
197 1,000 bp, 17,103 contigs were left. PyDamage was able to perform a successful damage estimation  
198 for 99.75% of these contigs (17,061 contigs). Because the ZSM028 sequencing library was not treated  
199 with uracil-DNA-glycosylase (Rohland et al., 2015), nor amplified with a damage suppressing DNA  
200 polymerase, we expect a relatively shallow DNA damage decay curve, and thus filtered for this using the  
201  $p_d^j$  parameter. We chose a prediction accuracy threshold of 0.67 after locating the knee point on Figure 5

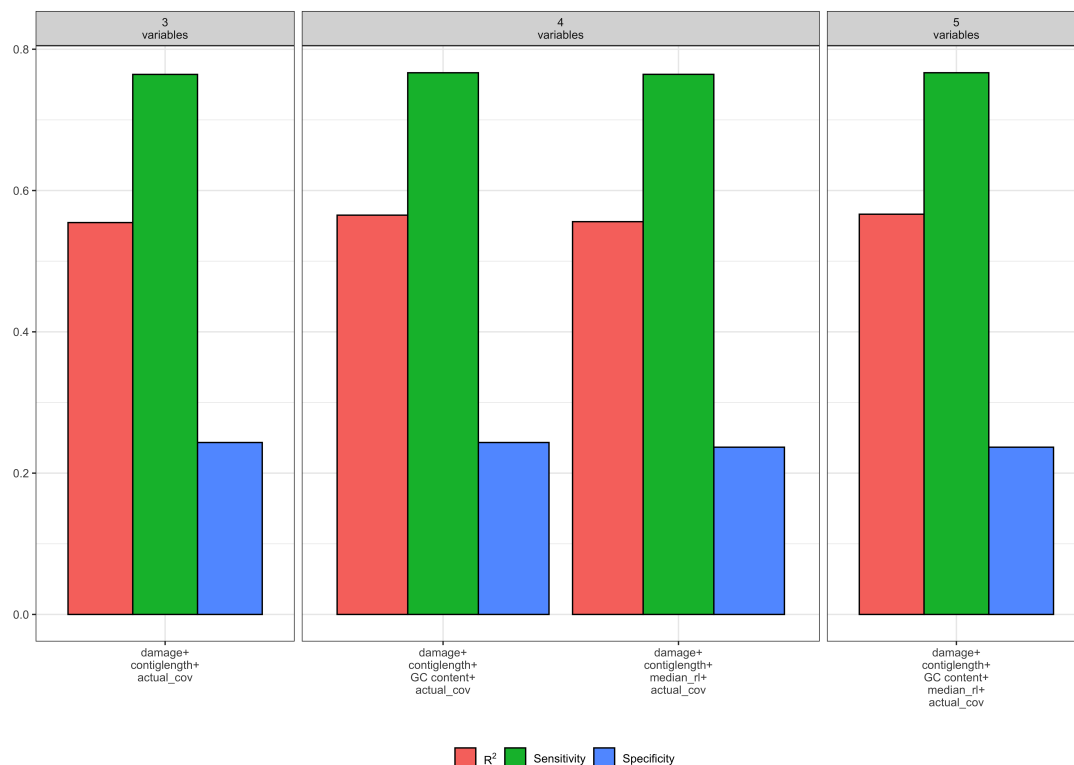


**Figure 2.** Measures of model fit calculated on the test data for three variables, four variables, and five variables, where red is Nagelkerke's  $R^2$ , green is model sensitivity and blue is model specificity. Model fit is not improved with the addition of variables beyond DNA damage, contig length, and contig coverage.

202 with the kneedle method (Satopaa et al., 2011). After filtering PyDamage results with a  $q$ -value  $\leq 0.05$ ,  
203  $p_d^j \leq 0.6$ , and *prediction accuracy*  $\geq 0.67$ , 1,944 contigs remain. The 5' damage for these contigs ranges  
204 from 4.0% to 45.1% with a mean of 14.3% (Figure 7). Their coverage spans 6.1X to 1,579.8X with a  
205 mean of 65.6X, while their length ranges from 1,002 bp to 90,306 bp with a mean of 5,212 bp and an  
206 N50 of 10,805 bp.

207 The Kraken2 taxonomic profile of the microbial contigs identified by PyDamage identified as ancient  
208 (Figure 6) is consistent with bacteria known to be members of the human gut microbiome, including  
209 *Prevotella* (239 contigs), *Treponema* (166 contigs), *Bacteroides* (103 contigs), *Lachnospiraceae* (119  
210 contigs) *Blautia* (36 contigs), *Ruminococcus* (25 contigs), *Phocaeicola* (18 contigs) and *Romboutsia*  
211 (16 contigs) (Schnorr et al., 2016; Pasolli et al., 2019; Singh et al., 2017), as well as taxonomic groups  
212 known to be involved in initial decomposition, such as *Clostridium* (145 contigs) (Hyde et al., 2017;  
213 Harrison et al., 2020; Dash and Das, 2020). In addition, eukaryotic contigs were assigned to humans (18  
214 contigs), and to the plant families Fabaceae (18 contigs) and Solanaceae (18 contigs), two families of  
215 economically important crops in the Americas that include beans, tomatoes, chile peppers, and tobacco.  
216 The remaining contigs were almost entirely assigned to higher taxonomic levels within the important  
217 gut microbiome phyla Bacteriodes, Firmicutes, Proteobacteria, and Spirochaetes, as well as to the  
218 Streptophyta phylum of vascular plants. Collectively, these 5 phyla accounted for 1283 of to 1494 contigs  
219 that could be taxonomically assigned.

220 Functional annotation of the authenticated ancient contigs using Prokka was successful for 1,901  
221 of 1,944 contigs. Among these, multiple genes of functional interest were identified, including contigs  
222 annotated as encoding the multidrug resistance proteins MdtA, MdtB, and MdtC, which convey, among  
223 other functions, bile salt resistance (Nagakubo et al., 2002) (Table 2). Kraken2 taxonomic profiling  
224 of these three contigs yields a taxonomic assignation to the gut spirochaete *Treponema succinifaciens*,  
225 a species absent in the gut microbiome of industrialized populations, but which is found globally in  
226 societies practicing traditional forms of subsistence (Obregon-Tito et al., 2015; Schnorr et al., 2014). Other

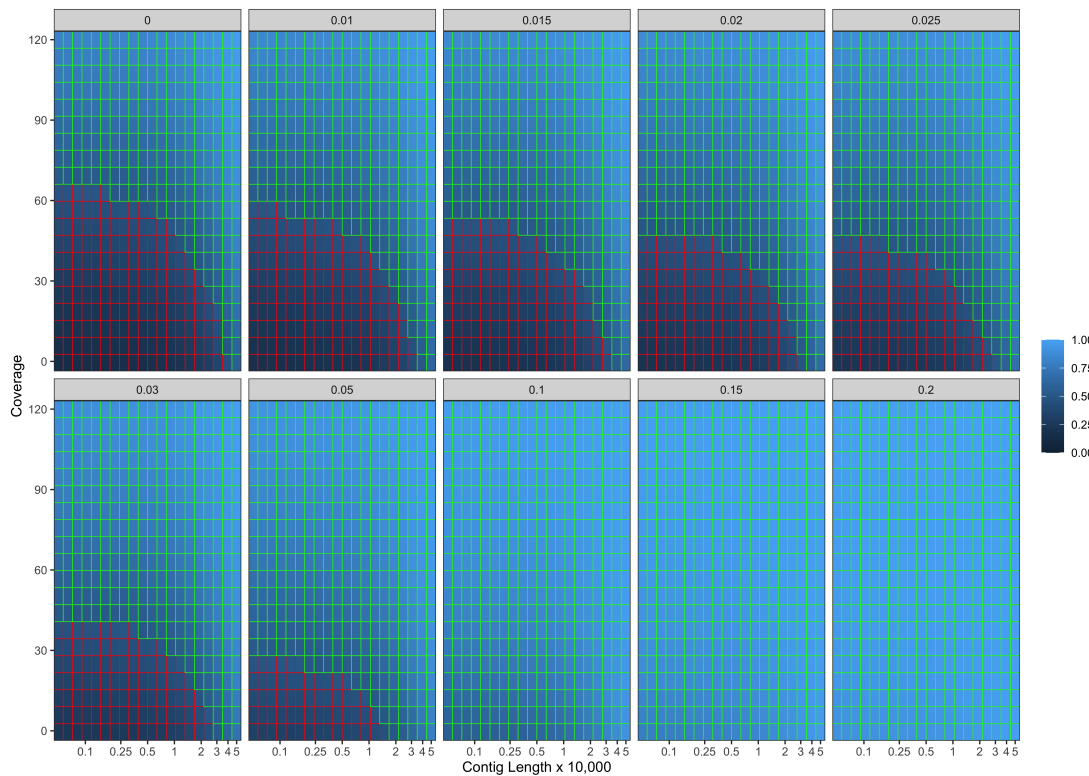


**Figure 3.** Predicted model accuracy of simulated data. Light blue indicates improved model accuracy, with parameter combinations resulting in better than 50% accuracy are outlined in green.

227 authenticated contigs contained genes associated with resistance to the natural antimicrobial compounds  
228 fosfomycin, colistin, daunorubicin/doxorubicin, tetracycline, polymyxin, and linearmycin. A growing  
229 body of evidence supports an ancient origin for resistance to most classes of natural antibiotics (D'Costa  
230 et al., 2011; Warinner et al., 2014; Christaki et al., 2020; Wibowo et al., 2021).

## 231 DISCUSSION AND CONCLUSION

232 *De novo* sequence assembly is increasingly being applied to ancient metagenomic data in order to improve  
233 lower rank taxonomic assignment and to enable functional profiling of ancient bacterial communities.  
234 The ability to reconstruct reference-free ancient genes, gene complexes, or even genomes opens the door  
235 to exploring microbial evolutionary histories and past functional diversity that may be underrepresented or  
236 absent in present-day microbial communities. A critical step in reconstructing this past diversity, however,  
237 is being able to distinguish DNA of ancient and modern origin (Warinner et al., 2017). Characteristic forms  
238 of damage that accumulate in DNA over time, such as DNA fragmentation and cytosine deamination,  
239 are widely used to authenticate aDNA (Orlando et al., 2021) and have been important, for example, in  
240 enabling the reconstruction of the Neanderthal genome from skeletal remains contaminated with varying  
241 levels of modern human DNA (Briggs et al., 2007a; Bokelmann et al., 2019; Peyrégne et al., 2019).

242 Nevertheless, applying such an approach to complex ancient microbial communities, such as archaeo-  
243 logical microbiome samples or sediments, is more challenging. Existing microbial reference sequences in  
244 databases such as NCBI RefSeq have been found to be insufficiently representative of modern microbial  
245 diversity (Pasolli et al., 2019; Manara et al., 2019), let alone ancient diversity, making reference-free *de*  
246 *novo* assembly particularly desirable for both modern and ancient microbial metagenomics. However, *de*  
247 *novo* assembly of aDNA has always been a challenge due to its highly fragmented nature. While tools  
248 have been designed to improve the assembly of ancient metagenomics data (Seitz and Nieselt, 2017),  
249 assessing the damage carried by the assembled contigs has remained an open problem. Although existing  
250 tools can determine the degree of aDNA damage for sequences mapped to a given reference sequence,  
251 scaling this up to accommodate the tens to hundreds of thousands of contig references generated by

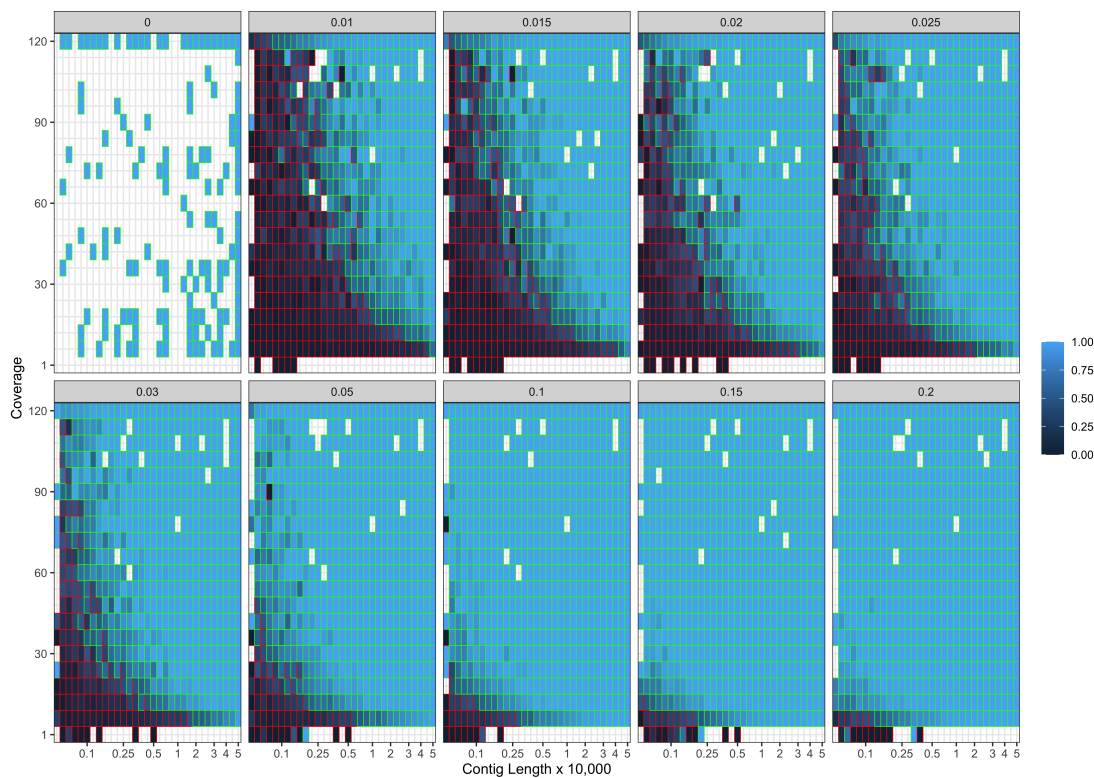


**Figure 4.** Observed model accuracy of simulated data. Light blue indicates improved model accuracy, with parameter combinations resulting in better than 50% accuracy are outlined with green lines. Grey tiles represent parameter combinations that were not sampled.

252 metagenomics assembly requires an alternative, automated approach to damage estimation.

253 Here, we have presented PyDamage as a tool to rapidly assess aDNA damage patterns for numerous  
254 reference sequences in parallel, allowing damage profiling of metagenome assembled contigs. To  
255 evaluate the performance of PyDamage model fitting and statistical testing, we benchmarked the tool  
256 using simulated assembly data of known coverage, length, GC content, read length, and damage level.  
257 While GC content and read length were not a major driver of the accuracy of PyDamage's predictions,  
258 reference length, coverage, and damage level each played major roles. Taken together, this three parameter  
259 combination greatly influenced the ability of PyDamage to make accurate damage assessments for a  
260 given contig. Overall, PyDamage has highly reliable damage prediction accuracy for contigs with high  
261 coverage, long lengths, and high damage, but the tool's power to assess damage is reduced for lower  
262 coverage, shorter contig lengths, and lower deamination damaged contigs. Although aDNA damage  
263 levels (cytosine deamination and fragmentation) are features of the DNA itself and out of the researcher's  
264 control, we show that researchers can generally improve model accuracy through deeper sequencing.

265 When comparing the parameter range of our simulated data to real world *de novo* assembly data,  
266 we find that some of PyDamage prediction accuracy limitations are mitigated by the assembly process  
267 itself: *de novo* assemblers usually need a minimum of approximately 5X coverage to assemble contigs  
268 (Figure 8) (Wibowo et al., 2021), and it is common practice to discard short contigs (<1000 bp) before  
269 further processing steps in a classical metagenomic *de novo* assembly analysis process. Nevertheless,  
270 low coverage, low damage, short contigs will remain a marginal challenge for damage characterization,  
271 even with further manual inspection. For example, for a 10,000 bp *de novo* assembled contig with 10%  
272 damage, PyDamage will only start to make reliable predictions once a coverage of 16X is reached (Figure  
273 3). For a similar contig with 20% damage, model accuracy is high even from 1X coverage. Overall, we  
274 find that PyDamage generally performs well on ancient metagenomic data with >5% damage, but contig  
275 length and coverage are also essential factors in determining the model accuracy for a given contig.

276 Although we used the kneedle method (Satopaa et al., 2011) to select the prediction accuracy threshold

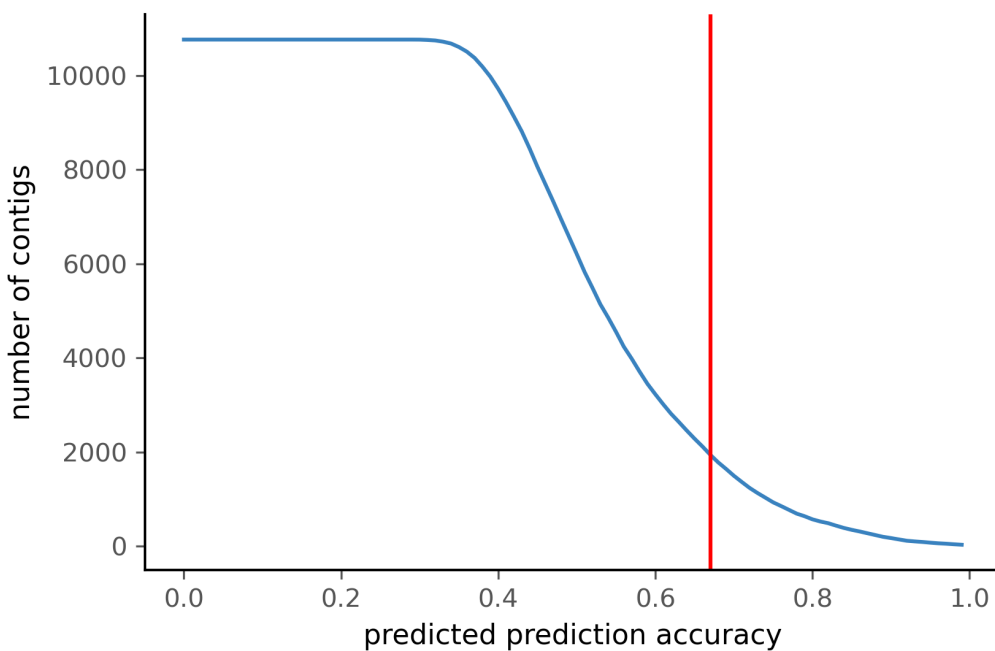


**Figure 5.** Number of ZSM028 contigs filtered by PyDamage with a  $q$ -value  $\leq 0.05$  as a function of the predicted prediction accuracy. In total, 12,271 of the 17,061 contigs were assigned  $q$ -value  $\leq 0.05$ .

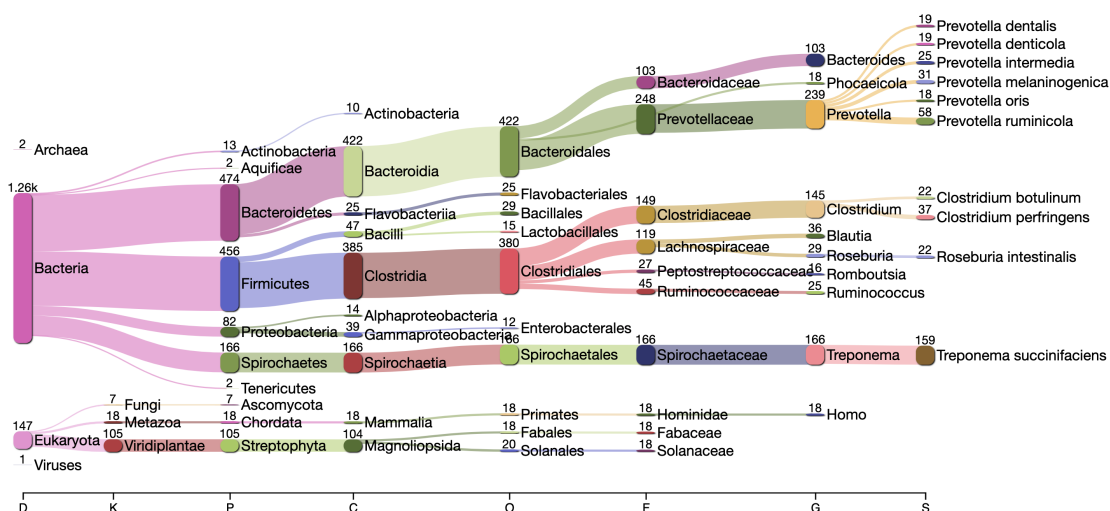


**Figure 6.** Taxonomic assignation by Kraken2 of the contigs filtered by PyDamage with  $q$ -value  $\leq 0.05$ ,  $p_d^j \leq 0.6$ , and  $\text{prediction accuracy} \geq 0.67$

for paleofeces sample ZSM028, users can adjust the selected prediction accuracy threshold according to the needs of their research question. For example, for some research questions where high accuracy in verifying damage is paramount, more stringent thresholds can be applied to minimize false positives, even though this increases false negatives. For other questions and where additional authentication criteria are available (such as taxonomic information or metagenomic bins), lower thresholds may be applied to reduce the number of false negatives due to insufficient coverage or contig length.

PyDamage is designed to estimate accumulated DNA damage in *de novo* assembled metagenomic sequences. However, although DNA damage can be used to authenticate DNA as ancient, it is important to

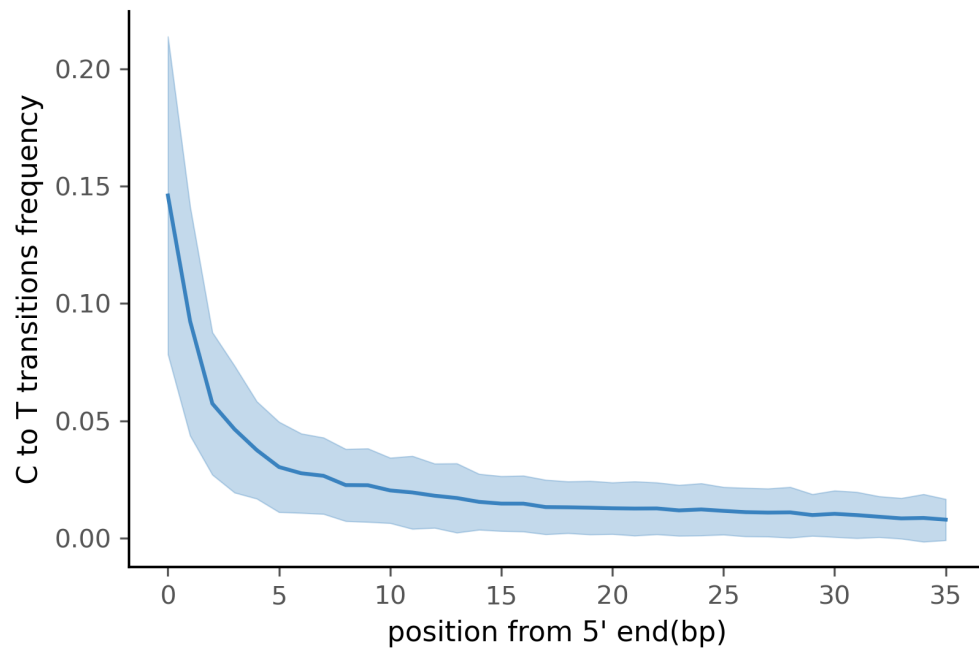


**Figure 7.** Damage profile of PyDamage filtered contigs of ZSM028. The center line is the mean, the shaded area is  $\pm$  one standard-deviation around the mean

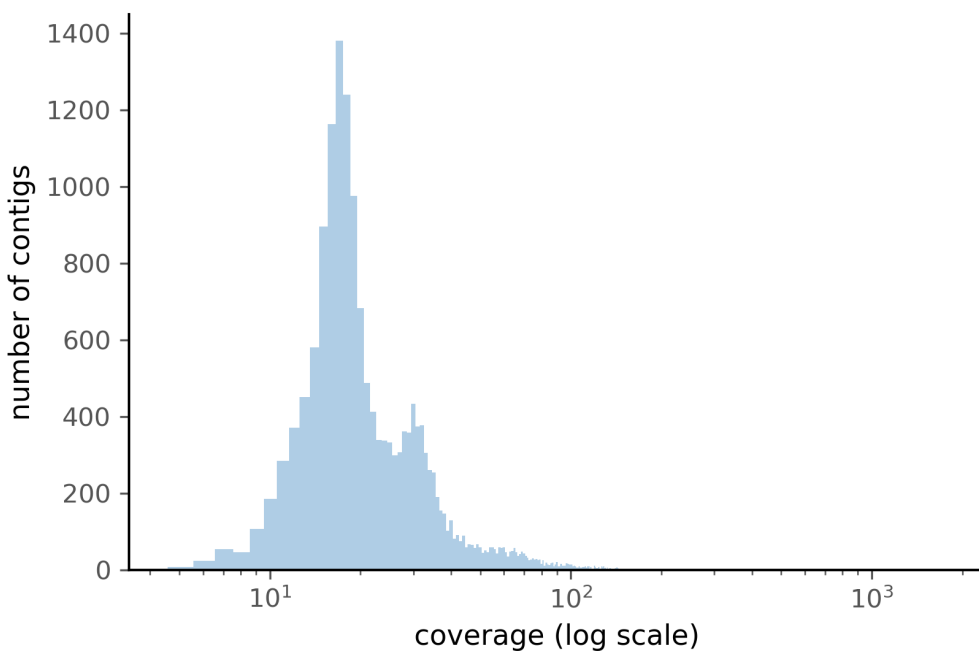


**Figure 8.** Distribution of the coverage for ZSM028 contigs  $>$  1,000 bp assembled by metaSPAdes.

285 note that it is not necessarily an indicator of *intra vitam* endogeneity. DNA within ancient remains typically  
286 consists of both an endogenous fraction present during life and an exogenous fraction accumulated

contig name	contig length (bp)	coverage	product
NODE_2446	3232	64.3	Arsenical-resistance protein Acr3
NODE_45	28638	26.0	Bifunctional polymyxin resistance protein ArnA
NODE_832	6259	46.3	Cobalt-zinc-cadmium resistance protein CzcA
NODE_832	6259	46.3	Cobalt-zinc-cadmium resistance protein CzcB
NODE_2661	3058	91.5	Colistin resistance protein EmrA
NODE_2661	3058	91.5	Colistin resistance protein EmrA
NODE_215	13020	27.0	Daunorubicin/doxorubicin resistance ATP-binding protein DrrA
NODE_136	16294	26.0	Daunorubicin/doxorubicin resistance ATP-binding protein DrrA
NODE_1676	4090	81.3	Fosmidomycin resistance protein
NODE_8410	1542	77.3	Linarmycin resistance ATP-binding protein LnrL
NODE_29	35207	27.8	Multidrug resistance ABC transporter ATP-binding and permease protein
NODE_232	12485	31.9	Multidrug resistance protein MdtA
NODE_97	19553	27.4	Multidrug resistance protein MdtA
NODE_12	45672	45.6	Multidrug resistance protein MdtA
NODE_10	46280	59.8	Multidrug resistance protein MdtA
NODE_97	19553	27.4	Multidrug resistance protein MdtB
NODE_97	19553	27.4	Multidrug resistance protein MdtB
NODE_12	45672	45.6	Multidrug resistance protein MdtC
NODE_10	46280	59.8	Multidrug resistance protein MdtC
NODE_232	12485	31.9	Multidrug resistance protein MdtC
NODE_17	41269	29.9	Multidrug resistance protein MdtK
NODE_465	8695	37.5	Tetracycline resistance protein TetO
NODE_204	13262	44.9	Tetracycline resistance protein, class C

**Table 2.** Contigs assembled by metaSPAdes, identified by PyDamage as carrying damage, and annotated as carrying resistance genes by Prokka

287 after death. For skeletal remains, the endogenous fraction typically consists of host DNA, as well  
 288 as possibly pathogen DNA if the host was infected at the time of death. For paleofeces or dental  
 289 calculus, the endogenous fraction typically consists of microbiome DNA, as well as trace amounts of  
 290 host, parasite, and dietary DNA. In both cases, the endogenous fraction of DNA is expected to carry DNA  
 291 damage accumulated since the death (skeletal remains, dental calculus) or defecation (paleofeces) of  
 292 the individual. Within the exogenous fraction, however, the DNA may span a range of ages. Nearly all  
 293 ancient remains undergo some degree of degradation and decomposition, during which either endogenous  
 294 (thanatotrichobiome) or exogenous (necrobiome) bacteria invade the remains and grow (Hyde et al.,  
 295 2017; Harrison et al., 2020; Dash and Das, 2020). DNA from bacteria that participated early in this  
 296 process (shortly after death or defecation), will carry similar levels of damage as the endogenous DNA  
 297 because they are of similar age. In contrast, more recent necrobiome activity will carry progressively less  
 298 age-related damage, and very recent sources of contamination from excavation, storage, curation, and  
 299 laboratory handling are expected to carry little to no DNA damage.

300 To demonstrate the utility of PyDamage on ancient metagenomic data, we applied PyDamage to  
 301 paleofeces ZSM028, a ca. 1300-year-old specimen of feces from a dry rockshelter site in Mexico that  
 302 was previously shown to have excellent preservation of endogenous gut microbiome DNA and low  
 303 levels of environmental contamination (Borry et al., 2020). Using PyDamage, we assessed the damage  
 304 profiles of contigs with lengths >1,000 bp, and authenticated nearly 2,000 contigs as carrying damage  
 305 patterns consistent with ancient DNA. The overwhelming majority of these contigs were consistent with  
 306 bacterial members of the human gut microbiome, as well as expected host and dietary components, but  
 307 a small fraction of authenticated contigs were assigned to environmental bacteria and fungi, including  
 308 the exogenous soil bacteria *Clostridium botulinum* (22 contigs) and *Clostridium perfringens* (38 contigs).  
 309 These taxa are known to be important early decomposers in the necrobiome (Harrison et al., 2020), and  
 310 the damage they carry suggests that they likely participated in the early degradation of the paleofeces  
 311 before decomposition was arrested by the extreme aridity of the rockshelter.

312 Among the PyDamage authenticated contigs assigned to gut-associated taxa, NODE\_10, NODE\_12,  
 313 and NODE\_97 are of particular interest. These contigs encode a multidrug resistant ABC (MdtABC)  
 314 transporter associated with bile salt resistance in the bacterium *T. succinifaciens*. *T. succinifaciens* is a  
 315 human-associated gut species that is today only found in the gut microbiomes of individuals engaging  
 316 in traditional forms of dietary subsistence (Obregon-Tito et al., 2015; Schnorr et al., 2014; Angelakis

317 et al., 2019). It is not found in the gut microbiomes of members of industrialized societies, and is believed  
318 extinct in these groups (Schnorr et al., 2016). Its identification within paleofeces provides insights into  
319 the evolutionary history of this enigmatic microorganism and its functional adaptation to the human gut  
320 (Schnorr et al., 2019). The additional identification of other resistance genes among the authenticated  
321 contigs provides further evidence regarding the evolution of antimicrobial resistance in human-associated  
322 microbes.

323 As the fields of microbiology and evolutionary biology increasingly turn to the archaeological record  
324 to investigate the rich and dynamic evolutionary history of ancient microbial communities, it has become  
325 vital to develop tools for assembling and authenticating ancient metagenomic DNA. Coupled with aDNA  
326 *de novo* assembly, PyDamage opens up new doors to explore and understand the functional diversity of  
327 ancient metagenomes.

328 **Code and Data availability**

- 329 • Genetic data for ZSM028 is available on the European Nucleotide Archive (ENA) under accession  
330 PRJEB33577.
- 331 • PyDamage Software and source code available from: [github.com/maxibor/pydamage](https://github.com/maxibor/pydamage), license:  
332 GPLv3
- 333 • The code to replicate the simulation of reads and contigs, and the figures is available in the following  
334 citable GitHub repository: DOI: 10.5281/zenodo.4630383 - [github.com/maxibor/pydamage-article](https://github.com/maxibor/pydamage-article)

335 **ACKNOWLEDGMENTS**

336 We thank Nigel Bean and Jonathon Tuke for extremely useful discussions. AH was funded by the Deutsche  
337 Forschungsgemeinschaft (DFG, German Research Foundation) under Germany's Excellence Strategy  
338 (EXC 2051 – Project-ID 390713860). ABR was funded by the European Research Council (ERC) under  
339 the European Union's Horizon 2020 research and innovation program under grant agreement no. 771234  
340 – PALEoRIDER. MB and CW were funded by the Werner Siemens Foundation ("Paleobiotechnology").

341 **REFERENCES**

- 342 Angelakis, E., Bachar, D., Yasir, M., Musso, D., Djossou, F., Gaborit, B., Brah, S., Diallo, A., Ndombe,  
343 G., Mediannikov, O., et al. (2019). Treponema species enrich the gut microbiota of traditional rural  
344 populations but are absent from urban individuals. *New microbes and new infections*, 27:14–21.
- 345 Babyak, M. A. (2004). What you see may not be what you get: a brief, nontechnical introduction to  
346 overfitting in regression-type models. *Psychosomatic medicine*, 66(3):411–421.
- 347 Benjamini, Y. and Hochberg, Y. (1995). Controlling the false discovery rate: a practical and powerful  
348 approach to multiple testing. *Journal of the Royal statistical society: series B (Methodological)*,  
349 57(1):289–300.
- 350 Bokelmann, L., Hajdinjak, M., Peyrégne, S., Brace, S., Essel, E., de Filippo, C., Glocke, I., Grote, S.,  
351 Mafessoni, F., Nagel, S., et al. (2019). A genetic analysis of the gibraltar neanderthals. *Proceedings of  
352 the National Academy of Sciences*, 116(31):15610–15615.
- 353 Borry, M., Cordova, B., Perri, A., Wibowo, M., Honap, T. P., Ko, J., Yu, J., Britton, K., Girdland-Flink,  
354 L., Power, R. C., Stuijts, I., Salazar-García, D. C., Hofman, C., Hagan, R., Kagoné, T. S., Meda, N.,  
355 Carabin, H., Jacobson, D., Reinhard, K., Lewis, C., Kostic, A., Jeong, C., Herbig, A., Hübner, A.,  
356 and Warinner, C. (2020). Coproid predicts the source of coprolites and paleofeces using microbiome  
357 composition and host dna content. *PeerJ*, 8:e9001. Publisher: PeerJ Inc.
- 358 Branch, M. A., Coleman, T. F., and Li, Y. (1999). A subspace, interior, and conjugate gradient method  
359 for large-scale bound-constrained minimization problems. *SIAM Journal on Scientific Computing*,  
360 21(1):1–23.
- 361 Brealey, J. C., Leitão, H. G., van der Valk, T., Xu, W., Bougiouri, K., Dalén, L., and Guschanski, K.  
362 (2020). Dental calculus as a tool to study the evolution of the mammalian oral microbiome. *Molecular  
363 biology and evolution*, 37(10):3003–3022.
- 364 Breitwieser, F. P. and Salzberg, S. L. (2016). Pavian: Interactive analysis of metagenomics data for  
365 microbiomics and pathogen identification. *bioRxiv*, page 084715.

- 366 Briggs, A. W., Stenzel, U., Johnson, P. L., Green, R. E., Kelso, J., Prüfer, K., Meyer, M., Krause, J.,  
367 Ronan, M. T., Lachmann, M., et al. (2007a). Patterns of damage in genomic dna sequences from a  
368 neandertal. *Proceedings of the National Academy of Sciences*, 104(37):14616–14621.
- 369 Briggs, A. W., Stenzel, U., Johnson, P. L. F., Green, R. E., Kelso, J., Prüfer, K., Meyer, M., Krause, J.,  
370 Ronan, M. T., Lachmann, M., and Pääbo, S. (2007b). Patterns of damage in genomic DNA sequences  
371 from a Neandertal. *Proceedings of the National Academy of Sciences*, 104(37):14616–14621.
- 372 Chan, M. (2020). *rwa: Perform a Relative Weights Analysis*. R package version 0.0.3.
- 373 Christaki, E., Marcou, M., and Tofarides, A. (2020). Antimicrobial resistance in bacteria: mechanisms,  
374 evolution, and persistence. *Journal of molecular evolution*, 88(1):26–40.
- 375 Compeau, P. E., Pevzner, P. A., and Tesler, G. (2011). How to apply de bruijn graphs to genome assembly.  
376 *Nature biotechnology*, 29(11):987–991.
- 377 Dabney, J., Meyer, M., and Pääbo, S. (2013). Ancient dna damage. *Cold Spring Harbor perspectives in  
378 biology*, 5(7):a012567.
- 379 Dash, H. R. and Das, S. (2020). Thanatomicobiome and epinecrotic community signatures for estimation  
380 of post-mortem time interval in human cadaver. *Applied Microbiology and Biotechnology*, pages 1–16.
- 381 D’Costa, V. M., King, C. E., Kalan, L., Morar, M., Sung, W. W., Schwarz, C., Froese, D., Zazula, G.,  
382 Calmels, F., Debruyne, R., et al. (2011). Antibiotic resistance is ancient. *Nature*, 477(7365):457–461.
- 383 Ginolhac, A., Rasmussen, M., Gilbert, M. T. P., Willerslev, E., and Orlando, L. (2011). mapDamage:  
384 testing for damage patterns in ancient DNA sequences. *Bioinformatics (Oxford, England)*, 27(15):2153–  
385 2155.
- 386 Hansen, H. B., Damgaard, P. B., Margaryan, A., Stenderup, J., Lynnerup, N., Willerslev, E., and Allentoft,  
387 M. E. (2017). Comparing ancient dna preservation in petrous bone and tooth cementum. *PloS one*,  
388 12(1):e0170940.
- 389 Harrison, L., Kooienga, E., Speights, C., Tomberlin, J., Lashley, M., Barton, B., and Jordan, H. (2020).  
390 Microbial succession from a subsequent secondary death event following mass mortality. *BMC  
391 microbiology*, 20(1):1–11.
- 392 Hofreiter, M., Jaenicke, V., Serre, D., Haeseler, A. v., and Pääbo, S. (2001). Dna sequences from multiple  
393 amplifications reveal artifacts induced by cytosine deamination in ancient dna. *Nucleic acids research*,  
394 29(23):4793–4799.
- 395 Huber, P. J. (1992). Robust estimation of a location parameter. In *Breakthroughs in statistics*, pages  
396 492–518. Springer.
- 397 Hyde, E. R., Metcalf, J. L., Bucheli, S. R., Lynne, A. M., and Knight, R. (2017). Microbial communities  
398 associated with decomposing corpses. *Forensic Microbiology, Wiley Online Books, John Wiley & Sons  
399 Ltd., The Atrium, Southern Gate, Chichester, West Sussex, UK*, pages 245–273.
- 400 Jónsson, H., Ginolhac, A., Schubert, M., Johnson, P. L. F., and Orlando, L. (2013). mapDamage2.0:  
401 fast approximate Bayesian estimates of ancient DNA damage parameters. *Bioinformatics (Oxford,  
402 England)*, 29(13):1682–1684.
- 403 Kang, D. D., Froula, J., Egan, R., and Wang, Z. (2015). Metabat, an efficient tool for accurately  
404 reconstructing single genomes from complex microbial communities. *PeerJ*, 3:e1165.
- 405 Langmead, B. and Salzberg, S. L. (2012). Fast gapped-read alignment with bowtie 2. *Nature methods*,  
406 9(4):357.
- 407 Li, H. and Durbin, R. (2009). Fast and accurate short read alignment with burrows–wheeler transform.  
408 *bioinformatics*, 25(14):1754–1760.
- 409 Manara, S., Asnicar, F., Beghini, F., Bazzani, D., Cumbo, F., Zolfo, M., Nigro, E., Karcher, N., Manghi,  
410 P., Metzger, M. I., et al. (2019). Microbial genomes from non-human primate gut metagenomes expand  
411 the primate-associated bacterial tree of life with over 1000 novel species. *Genome biology*, 20(1):1–16.
- 412 Mann, A. E., Sabin, S., Ziesemer, K., Vågene, Å. J., Schroeder, H., Ozga, A. T., Sankaranarayanan,  
413 K., Hofman, C. A., Yates, J. A. F., Salazar-García, D. C., et al. (2018). Differential preservation of  
414 endogenous human and microbial dna in dental calculus and dentin. *Scientific reports*, 8(1):1–15.
- 415 Meyer, M., Kircher, M., Gansauge, M.-T., Li, H., Racimo, F., Mallick, S., Schraiber, J. G., Jay, F.,  
416 Prüfer, K., De Filippo, C., et al. (2012). A high-coverage genome sequence from an archaic denisovan  
417 individual. *Science*, 338(6104):222–226.
- 418 Nagakubo, S., Nishino, K., Hirata, T., and Yamaguchi, A. (2002). The putative response regulator baer  
419 stimulates multidrug resistance of escherichia coli via a novel multidrug exporter system, mdtabc.  
420 *Journal of bacteriology*, 184(15):4161–4167.

- 421 Neukamm, J., Peltzer, A., and Nieselt, K. (2020). Damageprofiler: Fast damage pattern calculation for  
422 ancient dna. *BioRxiv*.
- 423 Nurk, S., Meleshko, D., Korobeynikov, A., and Pevzner, P. A. (2017). metaspades: a new versatile  
424 metagenomic assembler. *Genome research*, 27(5):824–834.
- 425 Obregon-Tito, A. J., Tito, R. Y., Metcalf, J., Sankaranarayanan, K., Clemente, J. C., Ursell, L. K., Xu,  
426 Z. Z., Van Treuren, W., Knight, R., Gaffney, P. M., et al. (2015). Subsistence strategies in traditional  
427 societies distinguish gut microbiomes. *Nature communications*, 6(1):1–9.
- 428 Orlando, L., Allaby, R., Skoglund, P., Der Sarkissian, C., Stockhammer, P. W., Ávila-Arcos, M. C., Fu, Q.,  
429 Krause, J., Willerslev, E., Stone, A. C., et al. (2021). Ancient dna analysis. *Nature Reviews Methods  
430 Primers*, 1(1):1–26.
- 431 Pasolli, E., Asnicar, F., Manara, S., Zolfo, M., Karcher, N., Armanini, F., Beghini, F., Manghi, P., Tett, A.,  
432 Ghensi, P., et al. (2019). Extensive unexplored human microbiome diversity revealed by over 150,000  
433 genomes from metagenomes spanning age, geography, and lifestyle. *Cell*, 176(3):649–662.
- 434 Peyrégne, S., Slon, V., Mafessoni, F., De Filippo, C., Hajdinjak, M., Nagel, S., Nickel, B., Essel, E.,  
435 Le Cabec, A., Wehrberger, K., et al. (2019). Nuclear dna from two early neandertals reveals 80,000  
436 years of genetic continuity in europe. *Science advances*, 5(6):eaaw5873.
- 437 pysam developers (2018). Pysam: a python module for reading and manipulating files in the sam/bam  
438 format.
- 439 R Core Team (2018). *R: A Language and Environment for Statistical Computing*. R Foundation for  
440 Statistical Computing, Vienna, Austria.
- 441 Renaud, G., Hanghøj, K., Willerslev, E., and Orlando, L. (2017). gargammel: a sequence simulator for  
442 ancient dna. *Bioinformatics*, 33(4):577–579.
- 443 Rho, M., Tang, H., and Ye, Y. (2010). Fraggenescan: predicting genes in short and error-prone reads.  
444 *Nucleic acids research*, 38(20):e191–e191.
- 445 Rohland, N., Harney, E., Mallick, S., Nordenfelt, S., and Reich, D. (2015). Partial uracil–dna–glycosylase  
446 treatment for screening of ancient dna. *Philosophical Transactions of the Royal Society B: Biological  
447 Sciences*, 370(1660):20130624.
- 448 Satopaa, V., Albrecht, J., Irwin, D., and Raghavan, B. (2011). Finding a "Kneedle" in a Haystack:  
449 Detecting Knee Points in System Behavior. In *2011 31st International Conference on Distributed  
450 Computing Systems Workshops*, pages 166–171, Minneapolis, MN, USA. IEEE.
- 451 Schnorr, S. L., Candela, M., Rampelli, S., Centanni, M., Consolandi, C., Basaglia, G., Turroni, S., Biagi,  
452 E., Peano, C., Severgnini, M., et al. (2014). Gut microbiome of the hadza hunter-gatherers. *Nature  
453 communications*, 5(1):1–12.
- 454 Schnorr, S. L., Hofman, C. A., Netshifhefhe, S. R., Duncan, F. D., Honap, T. P., Lesnik, J., and Lewis,  
455 C. M. (2019). Taxonomic features and comparisons of the gut microbiome from two edible fungus-  
456 farming termites (*macrotermes falciger*; *m. natalensis*) harvested in the vhembe district of limpopo,  
457 south africa. *BMC microbiology*, 19(1):1–22.
- 458 Schnorr, S. L., Sankaranarayanan, K., Lewis Jr, C. M., and Warinner, C. (2016). Insights into human evo-  
459 lution from ancient and contemporary microbiome studies. *Current opinion in genetics & development*,  
460 41:14–26.
- 461 Schubert, M., Lindgreen, S., and Orlando, L. (2016). AdapterRemoval v2: rapid adapter trimming,  
462 identification, and read merging. *BMC Research Notes*, 9:88.
- 463 Seabold, S. and Perktold, J. (2010). Statsmodels: Econometric and statistical modeling with python. In  
464 *9th Python in Science Conference*.
- 465 Seemann, T. (2014). Prokka: rapid prokaryotic genome annotation. *Bioinformatics (Oxford, England)*,  
466 30(14):2068–2069.
- 467 Seitz, A. and Nieselt, K. (2017). Improving ancient dna genome assembly. *PeerJ*, 5:e3126.
- 468 Singh, R. K., Chang, H.-W., Yan, D., Lee, K. M., Ucmak, D., Wong, K., Abrouk, M., Farahnik, B.,  
469 Nakamura, M., Zhu, T. H., et al. (2017). Influence of diet on the gut microbiome and implications for  
470 human health. *Journal of translational medicine*, 15(1):1–17.
- 471 Skoglund, P., Northoff, B. H., Shunkov, M. V., Derevianko, A. P., Pääbo, S., Krause, J., and Jakobsson, M.  
472 (2014). Separating endogenous ancient DNA from modern day contamination in a Siberian Neandertal.  
473 *Proceedings of the National Academy of Sciences*, 111(6):2229–2234.
- 474 Tett, A., Huang, K. D., Asnicar, F., Fehlner-Peach, H., Pasolli, E., Karcher, N., Armanini, F., Manghi,  
475 P., Bonham, K., Zolfo, M., et al. (2019). The prevotella copri complex comprises four distinct clades

- 476 underrepresented in westernized populations. *Cell host & microbe*, 26(5):666–679.
- 477 Virtanen, P., Gommers, R., Oliphant, T. E., Haberland, M., Reddy, T., Cournapeau, D., Burovski, E.,  
478 Peterson, P., Weckesser, W., Bright, J., van der Walt, S. J., Brett, M., Wilson, J., Jarrod Millman, K.,  
479 Mayorov, N., Nelson, A. R. J., Jones, E., Kern, R., Larson, E., Carey, C., Polat, İ., Feng, Y., Moore,  
480 E. W., Vand erPlas, J., Laxalde, D., Perktold, J., Cimrman, R., Henriksen, I., Quintero, E. A., Harris,  
481 C. R., Archibald, A. M., Ribeiro, A. H., Pedregosa, F., van Mulbregt, P., and Contributors, S. . . (2020).  
482 SciPy 1.0: Fundamental Algorithms for Scientific Computing in Python. *Nature Methods*, 17:261–272.
- 483 Warinner, C., Herbig, A., Mann, A., Fellows Yates, J. A., Weiß, C. L., Burbano, H. A., Orlando, L., and  
484 Krause, J. (2017). A robust framework for microbial archaeology. *Annual review of genomics and  
485 human genetics*, 18:321–356.
- 486 Warinner, C., Rodrigues, J. F. M., Vyas, R., Trachsel, C., Shved, N., Grossmann, J., Radini, A., Hancock,  
487 Y., Tito, R. Y., Fiddiment, S., et al. (2014). Pathogens and host immunity in the ancient human oral  
488 cavity. *Nature genetics*, 46(4):336–344.
- 489 Wibowo, M. C., Yang, Z., Borry, M., Hübner, A., Huang, K. D., Tierney, B. T., Zimmerman, S., Barajas-  
490 Olmos, F., Contreras-Cubas, C., García-Ortiz, H., Martínez-Hernández, A., Luber, J. M., Kirstahler, P.,  
491 Blohm, T., Smiley, F. E., Arnold, R., Ballall, S. A., Pamp, S. J., Russ, J., Maixner, F., Rota-Stabelli, O.,  
492 Segata, N., Reinhard, K., Orozco, L., Warinner, C., Snow, M., LeBlanc, S., and Kostic, A. D. (2021).  
493 Reconstruction of ancient microbial genomes from the human gut. *Nature*, *in press*, pages –.
- 494 Wood, D. E., Lu, J., and Langmead, B. (2019). Improved metagenomic analysis with kraken 2. *Genome  
495 biology*, 20(1):1–13.